Coupling of graphene and surface plasmons

Norman J. Morgenstern Horing
Department of Physics & Engineering Physics, Stevens Institute of Technology, Hoboken, New Jersey 07030, USA
(Received 20 April 2009; revised manuscript received 9 July 2009; published 2 November 2009)

We analyze the plasmon spectrum of a graphene sheet in the vicinity of a thick plasmalike substrate, finding linear dispersion in some parameter ranges.

DOI: 10.1103/PhysRevB.80.193401 PACS number(s): 52.40.−w, 94.30.ct, 94.20.wf, 52.35.−g

I. INTRODUCTION

Recent intensive research[1–6] on the plasmon spectrum in carbon nanotubes and graphene has revealed a linear π plasmon dispersion relation, which plays an important role in the response of these materials to experimental probes of their properties. Kramberger *et al.*[1] ascribe this linear plasmon dispersion to local field effects. In this Brief Report we examine other possible sources of linear plasmon dispersion in graphene, which may arise from interaction of the native graphene plasmon ($\omega \sim q^{1/2}$) with the surface plasmon of a nearby thick substrate hosting a plasma taken to be semi-infinite (Fig. 1). The parallel two-dimensional (2D) plasma of the graphene sheet alone has been thoroughly examined,[7–11] and here, we study the effects of the Coulomb interaction of the 2D graphene plasma with the semi-infinite plasma of the nearby thick substrate,[12–14] whose local surface plasmon is given by $\omega_s = \omega_p/\sqrt{2}$ ($\omega_p^2 = 4\pi e^2 \rho_{3D}/m$; ρ_{3D} is the bulk electron density of the substrate), which is devoid of linear character. However, the coupling of the graphene sheet (at $z_0 < 0$), which supports a two-dimensional plasma parallel to the surface, with the semi-infinite plasmalike medium somewhat removed from it, can induce linearity into the plasmon dispersion at low wave number q. (Of course, such a mechanism for linear plasmon dispersion is not available for *isolated* graphene.)

The fullest description of such physical features is provided by the dynamic, nonlocal, and spatially inhomogeneous screening function, $K(\mathbf{r}_1,t_1;\mathbf{r}_2,t_2)$, which is the space-time matrix inverse of the direct dielectric function $\varepsilon(\mathbf{r}_1,t_1;\mathbf{r}_2,t_2)$ of the system

$$\int d^{(3)}\mathbf{x} \int d\tau K(\mathbf{r}_1,t_1;\mathbf{x},\tau)\varepsilon(\mathbf{x},\tau;\mathbf{r}_2,t_2) = \delta^{(3)}(\mathbf{r}_1-\mathbf{r}_2)\,\delta(t_1-t_2). \tag{1}$$

The frequency poles of $K(\mathbf{r}_1,\mathbf{r}_2;\omega)$ define the plasmon modes of the system and the residues describe the relative excitation amplitudes (oscillator strengths) of these modes. Rewriting Eq. (1) in the form of an integral equation, we note that

$$\varepsilon(\mathbf{r},t;\mathbf{r}',t') = \delta^{(3)}(\mathbf{r}-\mathbf{r}')\,\delta(t-t') + \alpha(\mathbf{r},t;\mathbf{r}',t'), \tag{2}$$

where $\alpha(\mathbf{r},t;\mathbf{r}',t')$ is the combined polarizability of the semi-infinite and two-dimensional plasma constituents of the system. Thus, Eqs. (1) and (2) lead to

$$K(\mathbf{r}_1,t_1;\mathbf{r}_2,t_2) = \delta^{(3)}(\mathbf{r}_1-\mathbf{r}_2)\,\delta(t_1-t_2) - \int d^{(3)}\mathbf{x} \int d\tau \alpha(\mathbf{r}_1,t_1;\mathbf{x},\tau)K(\mathbf{x},\tau;\mathbf{r}_2,t_2). \tag{3}$$

Furthermore, when the energies of the quantum-well bound state and the continuum of extended states of the bulk are well separated (and transitions between them are energetically inaccessible),[15] it is an accurate and useful approximation to write the combined polarizability, $\alpha(\mathbf{r}_1,t_1;\mathbf{r}_2,t_2)$, as the sum of the polarizabilities of the semi-infinite plasma, $\alpha_{semi}(\mathbf{r}_1,t_1;\mathbf{r}_2,t_2)$, and the two-dimensional plasma, $\alpha_{2D}(\mathbf{r}_1,t_1;\mathbf{r}_2,t_2)$, with the result

$$\begin{aligned} K(\mathbf{r}_1,t_1;\mathbf{r}_2,t_2) &+ \int d^{(3)}\mathbf{x} \int d\tau \alpha_{semi}(\mathbf{r}_1,t_1;\mathbf{x},\tau)K(\mathbf{x},\tau;\mathbf{r}_2,t_2) \\ &= \delta^{(3)}(\mathbf{r}_1-\mathbf{r}_2)\,\delta(t_1-t_2) \\ &\quad - \int d^{(3)}\mathbf{x} \int d\tau \alpha_{2D}(\mathbf{r}_1,t_1;\mathbf{x},\tau)K(\mathbf{x},\tau;\mathbf{r}_2,t_2). \end{aligned} \tag{4}$$

Alternatively, the left-hand side of Eq. (4) may be written as

$$\begin{aligned} &\int d^{(3)}\mathbf{x} \int d\tau \varepsilon_{semi}(\mathbf{r}_1,t_1;\mathbf{x},\tau)K(\mathbf{x},\tau;\mathbf{r}_2,t_2) \\ &\quad = \delta^{(3)}(\mathbf{r}_1-\mathbf{r}_2)\,\delta(t_1-t_2) \\ &\qquad - \int d^{(3)}\mathbf{x} \int d\tau \alpha_{2D}(\mathbf{r}_1,t_1;\mathbf{x},\tau)K(\mathbf{x},\tau;\mathbf{r}_2,t_2), \end{aligned} \tag{5}$$

where ε_{semi} has the space-time matrix inverse K_{semi}, which is the screening function of the semi-infinite medium alone

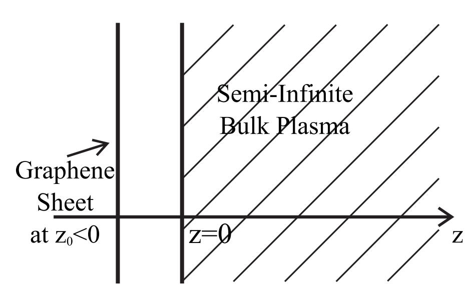

FIG. 1. Schematic of the geometry considered.

$$\int d^{(3)}\mathbf{x}\int d\tau K_{semi}(\mathbf{r}_1,t_1;\mathbf{x},\tau)\varepsilon_{semi}(\mathbf{x},\tau;\mathbf{r}_2,t_2) = \delta^{(3)}(\mathbf{r}_1-\mathbf{r}_2)\delta(t_1-t_2), \quad (6)$$

in full analogy to Eq. (1). Accordingly, Eq. (5) implies that

$$K(\mathbf{r}_1,t_1;\mathbf{r}_2,t_2) = K_{semi}(\mathbf{r}_1,t_1;\mathbf{r}_2,t_2) - \int d^{(3)}\mathbf{x}\int d\tau\int d^{(3)}\mathbf{x}'\int d\tau' K_{semi}(\mathbf{r}_1,t_1;\mathbf{x},\tau) \times\alpha_{2\mathrm{D}}(\mathbf{x},\tau;\mathbf{x}',\tau')K(\mathbf{x}',\tau',\mathbf{r}_2,t_2). \quad (7)$$

II. SOLUTION OF THE INTEGRAL EQUATION

For a semi-infinite bulk plasma and a nearby parallel 2D graphene sheet plasma, we Fourier transform in the surface plane of translational invariance ($\bar{\mathbf{r}}_1-\bar{\mathbf{r}}_2\to\bar{\mathbf{q}}$, where $\mathbf{r}=\bar{\mathbf{r}},z$) and time ($t_1-t_2\to\omega$), obtaining (suppress $\bar{\mathbf{q}},\omega$),

$$K(z_1,z_2) = K_{semi}(z_1,z_2) - \int dz_3\int dz_4 K_{semi}(z_1,z_3)\alpha_{2\mathrm{D}}(z_3,z_4)K(z_4,z_2). \quad (8)$$

We have previously shown that the dynamic, nonlocal, and spatially inhomogeneous screening function of the semi-infinite medium (occupying $z=0\to\infty$) is given by[16] [$\theta(z)=1$ for $z>0$; 0 for $z<0$; 1/2 for $z=0$]

$$\begin{aligned}K_{semi}(z_1,z_2) = {}&\theta(-z_1)\left[\delta(z_1-z_2)-\frac{\varepsilon_{\bar{q}}}{1+\varepsilon_{\bar{q}}}e^{|\bar{q}|z_1}\delta(z_2) + \frac{2\varepsilon_{\bar{q}}}{1+\varepsilon_{\bar{q}}}K_0(z_2)e^{|\bar{q}|z_1}\theta(z_2)\right]\\ &+\theta(z_1)\left\{\nu_0(z_1)\left[\frac{|\bar{q}|\varepsilon_{\bar{q}}}{1+\varepsilon_{\bar{q}}}\delta(z_2) - \frac{2|\bar{q}|\varepsilon_{\bar{q}}}{1+\varepsilon_{\bar{q}}}K_0(z_2)\theta(z_2)\right]\right\}\\ &+\theta(z_1)[K_0(z_1+z_2)+K_0(z_1-z_2)]\theta(z_2),\end{aligned} \quad (9)$$

where $\varepsilon_0(q_z,\bar{q};\omega)$ is the bulk dielectric function of the semi-infinite medium and

$$K_0(z_2) = (1/\pi)\int_0^\infty dq_z\cos(q_z z_2)[\varepsilon_0(q_z,\bar{q};\omega)]^{-1}, \quad (10)$$

and

$$\nu_0(z_2) = (2/\pi)\int_0^\infty dq_z\cos(q_z z_2)[(q_z^2+|\bar{q}|^2)\varepsilon_0(q_z,\bar{q};\omega)]^{-1}, \quad (11)$$

with $\varepsilon_{\bar{q}}^{-1}=|\bar{q}|\nu_0(0)$. We further define

$$J(z_0) = \int dz_3 K_{semi}(z_0,z_3)e^{-|\bar{q}|z_3}. \quad (12)$$

For the thin 2D sheet of graphene located at z_0, the three-dimensional polarizability is described by[17]

$$\alpha_{2\mathrm{D}}(z_1,z_2) = \delta(z_2-z_0)e^{-|\bar{q}|(z_1-z_0)}\alpha_{2\mathrm{D}}, \quad (13)$$

with the last factor on the right of Eq. (13), $\alpha_{2\mathrm{D}}=\alpha_{2\mathrm{D}}(\bar{\mathbf{q}},\omega)$, as the planar 2D polarizablilty on the graphene sheet in 2D wave-vector frequency representation. With this, we have solved the integral equation for the combined screening function of the two-component system, Eq. (8), *exactly* in closed form as

$$K(z_1,z_2) = K_{semi}(z_1,z_2) - \frac{\alpha_{2\mathrm{D}}e^{|\bar{q}|z_0}J(z_1)K_{semi}(z_0,z_2)}{1+\alpha_{2\mathrm{D}}e^{|\bar{q}|z_0}J(z_0)}. \quad (14)$$

III. GRAPHENE PLASMON IN INTERACTION WITH SURFACE PLASMON

Considering the local limit, we have $\varepsilon_{\bar{q}}=\varepsilon_0(\omega)$ for the semi-infinite medium, and

$$K_0(z_2) = \delta(z_2)/\varepsilon_0(\omega), \quad (15)$$

with

$$\nu_0(z_2) = e^{-|\bar{q}||z_2|}/[|\bar{q}|\varepsilon_0(\omega)]. \quad (16)$$

This leads to $K_{semi}(z_1,z_2)$ in the local limit as[16]

$$\begin{aligned}K_{semi}(z_1,z_2) = {}&\theta(-z_1)\left\{\delta(z_1-z_2)+\delta(z_2)e^{|\bar{q}|z_1}\left(\frac{1-\varepsilon_0(\omega)}{1+\varepsilon_0(\omega)}\right)\right\}\\ &+\theta(z_1)\left\{\frac{\delta(z_1-z_2)}{\varepsilon_0(\omega)} + \delta(z_2)e^{-|\bar{q}|z_1}\frac{1}{\varepsilon_0(\omega)}\left(\frac{\varepsilon_0(\omega)-1}{\varepsilon_0(\omega)+1}\right)\right\}.\end{aligned} \quad (17)$$

The plasmon dispersion relation for the coupled system of the graphene sheet and the nearby semi-infinite plasma is given by the frequency poles of the second term on the right of Eq. (14), namely,

$$1+\alpha_{2\mathrm{D}}e^{|\bar{q}|z_0}J(z_0) = 0. \quad (18)$$

Determining $J(z_0)$ using Eq. (12) in the local limit of $K_{semi}(z_0,z_3)$ given by Eq. (17), we have

$$1+\alpha_{2\mathrm{D}}\left(1+e^{2|\bar{q}|z_0}\left[\frac{1-\varepsilon_0}{1+\varepsilon_0}\right]\right) = 0, \quad (19)$$

where $\varepsilon_0=1-\omega_p^2/\omega^2$ for the local limit of the bulk dielectric function of the semi-infinite medium and $\alpha_{2\mathrm{D}}=-\omega_{2\mathrm{D}}^2/\omega^2$ for the graphene sheet. In this analysis we first consider only intraband polarizability terms for doped graphene since we seek long wavelength modes $\omega\sim q$ at low wave numbers, and interband contributions to the polarizability are relatively small for such low frequency, low wave number terms with $\hbar\omega_{2\mathrm{D}}/\mu\ll 2$, μ being the Fermi energy; following this we examine the role of interband corrections to the polarizability approximately. Here, the local graphene plasma frequency is given by[7–11]

$$\omega_{2D}^2 = \omega_{Gr}^2 = \lambda^2 |\bar{q}|, \tag{20}$$

where

$$\lambda^2 = \gamma e^2 \sqrt{4\pi\rho_{2D}}/\hbar, \tag{21}$$

with γ as the effective Fermi velocity and ρ_{2D} is the 2D sheet density. Thus, the plasma frequency for graphene depends on the sheet density as $\rho_{2D}^{1/4}$, in contrast to usual $\rho_{2D}^{1/2}$ dependence.[11] With these remarks in view, Eq. (19) yields

$$\omega^2 = \omega_{2D}^2 \left(1 + e^{2|\bar{q}|z_0} \frac{\omega_p^2}{2\omega^2 - \omega_p^2} \right). \tag{22}$$

The two coupled plasmon frequencies given by the roots of Eq. (22) are ($\omega_s^2 = \omega_p^2/2$)

$$\omega_{\pm}^2 = \tfrac{1}{2}[\omega_s^2 + \omega_{2D}^2] \pm \tfrac{1}{2}\sqrt{[\omega_s^2 + \omega_{2D}^2]^2 - 4\omega_s^2\omega_{2D}^2[1 - e^{2|\bar{q}|z_0}]}. \tag{23}$$

For large separation, $|\bar{q}||z_0| \gg 1$, the two plasmons decouple completely, as

$$\omega_+^2 = \omega_s^2 \quad \text{and} \quad \omega_-^2 = \omega_{2D}^2, \tag{24}$$

whereas the two modes are fully hybridized for zero separation, $|\bar{q}|z_0 \to 0$

$$\omega_+^2 = \omega_s^2 + \omega_{2D}^2 \quad \text{and} \quad \omega_-^2 = 0. \tag{25}$$

If wave number is also low in the sense that $\omega_{2D}^2 = \lambda^2|\bar{q}| \ll \omega_s^2$, the ω_+ plasmon is, approximately,

$$\omega_+ = \omega_s + \frac{1}{2}\frac{\lambda^2|\bar{q}|}{\omega_s}, \tag{26}$$

which is linear in $|\bar{q}|$, but *not* acoustic.

For arbitrary ω_{2D}^2/ω_s^2, and low but nonzero values of $|\bar{q}||z_0| \ll 1$ (recall that z_0 is negative), we have

$$\omega_+^2 = [\omega_s^2 + \omega_{2D}^2] - \frac{2\omega_s^2\omega_{2D}^2}{[\omega_s^2 + \omega_{2D}^2]}|\bar{q}||z_0|, \tag{27}$$

in which the coupling hybridization of the two modes is somewhat diminished, and

$$\omega_-^2 = \frac{2\omega_s^2\omega_{2D}^2}{[\omega_s^2 + \omega_{2D}^2]}|\bar{q}||z_0|, \tag{28}$$

which is not specifically an acoustic mode because $\omega_{2D}^2 \sim |\bar{q}|$ is involved in the denominator on the right of Eq. (28), as well as in the numerator. For very low wave numbers, $\omega_{2D} \ll \omega_s$, the mode ω_- is acoustic with

$$\omega_-^2 \cong 2\omega_{2D}^2|\bar{q}||z_0| \sim |\bar{q}|^2. \tag{29}$$

However, when $\omega_{2D} \gg \omega_s$, it is not acoustic, having the value

$$\omega_-^2 \cong 2\omega_s^2|\bar{q}||z_0| \sim |\bar{q}|. \tag{30}$$

To assess the role of interband corrections, we note that the ratio, R, of interband terms to intraband terms in the graphene polarizability is given by[7–11]

$$R = \frac{\hbar\omega}{4\mu}\left(ln \left| \frac{1 - \hbar\omega/2\mu}{1 + \hbar\omega/2\mu} \right| \right) \cong -\left(\frac{\hbar\omega}{2\mu}\right)^2, \tag{31}$$

where $\hbar\omega/2\mu \ll 1$ as discussed above. Accordingly, the polarizability is approximately given by

$$\alpha_{2D} = -\frac{\omega_{2D}^2}{\omega^2} + \left(\frac{\hbar\omega_{2D}}{2\mu}\right)^2 \equiv -\frac{\omega_{2D}^2}{\omega^2} + \beta \tag{32}$$

and we have defined β as

$$\beta \equiv \left(\frac{\hbar\omega_{2D}}{2\mu}\right)^2 \ll 1. \tag{33}$$

(For example, with $|\bar{q}| = 0.1q_F$ [Fermi wave number], β is about 0.04.) The resulting graphene-coupled plasmon dispersion relation, Eq. (19), may be rewritten as

$$[1 + \beta]\omega^4 - \omega^2[\omega_{2D}^2 + \omega_s^2(1 + \beta\xi)] + \omega_{2D}^2\omega_s^2\xi = 0, \tag{34}$$

where ξ is defined by

$$\xi = 1 - e^{2|\bar{q}|z_0}. \tag{35}$$

The solutions of the quadratic dispersion relation are given by

$$\omega_{\pm}^2 = \frac{[\omega_{2D}^2 + \omega_s^2(1 + \beta\xi)]}{2(1 + \beta)} \pm \frac{\sqrt{(\omega_{2D}^2 + \omega_s^2[1 + \beta\xi])^2 - 4(1 + \beta)\omega_{2D}^2\omega_s^2\xi}}{2(1 + \beta)}. \tag{36}$$

The plasmons decouple as $z_0 \to -\infty$ ($\xi \to 1$) with the results

$$\omega_+^2 = \frac{\omega_{2D}^2}{1 + \beta} \quad \text{and} \quad \omega_-^2 = \omega_s^2, \tag{37}$$

showing that the graphene mode is lowered somewhat by the intersubband contribution, while the decoupled semi-infinite bulk surface plasmon is unaffected by it. On the other hand, when the graphene sheet is directly on the bounding surface of the bulk, $z_0 = 0$ and $\xi = 0$, we obtain

$$\omega_+^2 = \frac{\omega_{2D}^2 + \omega_s^2}{1 + \beta} \quad \text{and} \quad \omega_-^2 = 0, \tag{38}$$

showing that the fully coupled plasma modes are equally affected by the intersubband contribution in this case. Finally, considering z_0 small in the sense that

$$2|\bar{q}|z_0 \ll 1, \quad \text{or} \quad \xi = -2|\bar{q}|z_0, \tag{39}$$

we have

$$\omega_{\pm}^2 = \frac{(\omega_{2D}^2 + \omega_s^2[1 - 2\beta z_0|\bar{q}|])}{2(1 + \beta)} \pm \frac{\sqrt{(\omega_{2D}^2 + \omega_s^2[1 - 2\beta z_0|\bar{q}|])^2 + 8(1 + \beta)\omega_{2D}^2\omega_s^2 z_0|\bar{q}|}}{2(1 + \beta)}. \tag{40}$$

This result may be further expanded to examine particular limits as done above. However, as $\beta = (\hbar\omega_{2D}/2\mu)^2 \ll 1$, no significant deviations are to be expected.

IV. SUMMARY: DISCUSSION

The formulation of this calculation in Sec. II, including Eqs. (8)–(14), is sufficiently general to accommodate detailed studies of a graphene sheet near a thick substrate ranging from the *nonlocal* plasmon spectrum to static shielding, including an ambient magnetic field if desired. Furthermore, we have presented the exact, explicit solution for the screening function in closed form [Eq. (14)], and examined its frequency poles [Eq. (18)] to determine the coupled plasmon mode spectrum. The local results that we have obtained indicate that complete hybridization of the two plasmon modes, ω_s and ω_{2D}, occurs when the 2D graphene sheet is directly on the bounding surface of the bulk medium, $z_0=0$. The completely hybridized upper mode at $z_0=0$ exhibits linear dispersion [Eq. (26)] for wave number low in the sense $\omega_{2D}^2 \ll \omega_s^2$ but it is not acoustic.

The mode coupling is reduced when the 2D sheet is not exactly at $z_0=0$, and explicit results for the upper and lower partially coupled modes are presented in Eqs. (27) and (28) for small, but finite, separation, $|\bar{q}||z_0|<1$. The lower mode is not always an acoustic mode, although it becomes acoustic when $\omega_{2D} \ll \omega_s$. Of course, the two modes decouple completely for large separation, $|\bar{q}||z_0| \gg 1$. Finally, we have also examined the role of interband (as well as intraband) polarizability terms in the coupled plasmon modes in Eqs. (30)–(40), finding it to be small.

ACKNOWLEDGMENT

The author gratefully acknowledges support for this work by DARPA under Grant No. HR0011-09-1-0008.

[1] C. Kramberger, R. Hambach, C. Giorgetti, M. H. Rümmeli, M. Knupfer, J. Fink, B. Büchner, L. Reining, E. Einarsson, S. Maruyama, F. Sottile, K. Hannewald, V. Olevano, A. G. Marinopoulos, and T. Pichler, Phys. Rev. Lett. **100**, 196803 (2008).

[2] T. Eberlein, U. Bangert, R. R. Nair, R. Jones, M. Gass, A. L. Bleloch, K. S. Novoselov, A. Geim, and P. R. Briddon, Phys. Rev. B **77**, 233406 (2008).

[3] O. Stephan, D. Taverna, M. Kociak, K. Suenaga, L. Henrard, and C. Colliex, Phys. Rev. B **66**, 155422 (2002).

[4] D. Taverna, M. Kociak, V. Charbois, and L. Henrard, Phys. Rev. B **66**, 235419 (2002).

[5] D. Taverna, M. Kociak, O. Stephan, A. Fabre, E. Finot, B. Decamps, and C. Colliex, Phys. Rev. Lett. **100**, 035301 (2008).

[6] P. E. Trevisanutto, C. Giorgetti, L. Reining, M. Ladisa, and V. Olevano, Phys. Rev. Lett. **101**, 226405 (2008).

[7] K. W.-K. Shung, Phys. Rev. B **34**, 979 (1986).

[8] K. W.-K. Shung, Phys. Rev. B **34**, 1264 (1986).

[9] T. Ando, J. Phys. Soc. Jpn. **75**, 074716 (2006).

[10] B. Wunsch, T. Stauber, F. Sols, and F. Guinea, New J. Phys. **8**, 318 (2006).

[11] E. H. Hwang and S. DasSarma, Phys. Rev. B **75**, 205418 (2007).

[12] N. J. M. Horing, T. Jena, H. L. Cui, and J. D. Mancini, Phys. Rev. B **54**, 2785 (1996).

[13] M. F. Lin, C. S. Huang, and D. S. Chuu, Phys. Rev. B **55**, 13961 (1997).

[14] A. V. Chaplik, Sov. Phys. JETP **35**, 395 (1972).

[15] N. J. M. Horing, G. Gumbs, and T. Park, Physica B **299**, 165 (2001).

[16] N. J. M. Horing, E. Kamen, and H. L. Cui, Phys. Rev. B **32**, 2184 (1985).

[17] N. J. M. Horing, H. C. Tso, and G. Gumbs, Phys. Rev. B **36**, 1588, (1987).